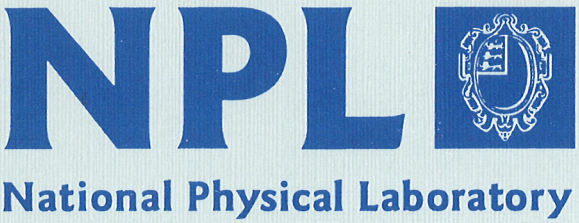
CMMT(A)22



Methods of Predicting Oxide Spallation and the Influence of Substrate Geometry

H E Evans

April 1996

The National Physical Laboratory is operated on behalf of the DTI by NPL Management Limited, a wholly owned subsidiary of Serco Group plc

CMMT(A)22
April 1996

Methods of Predicting Oxide Spallation and the Influence of Substrate Geometry

H E Evans
Consultant
Bilston
Ashleworth
GL19 4HX

ABSTRACT

Much progress has been made in the last decade or so in understanding the mechanisms of oxide spallation from flat substrates and in the use of numerical modelling to predict the critical temperature drop to initiate spallation. Key elements of this body of work are reviewed in this paper. Additionally, the application of present understanding to spallation from curved substrates is considered. Although there is reasonable qualitative understanding of the likely processes involved, the ability to quantify mechanisms and predict spallation from such substrates is much less developed than for flat substrates. The situation reflects a paucity of experimental information on the cracking processes leading to spallation, on the kinetics of spallation during cooling and also on the development of oxidation growth stresses on curved substrates. The paper concludes by highlighting broad directions for future research work.

© Crown copyright 1996
Reproduced by permission of the Controller of HMSO

ISSN 1361-4061

National Physical Laboratory
Teddington, Middlesex, United Kingdom, TW11 0LW

No extracts from this report may be reproduced without
the prior written consent of the Managing Director,
National Physical Laboratory; the source must be acknowledged.

Approved on behalf of Managing Director, NPL, by Dr M K Hossain,
Director, Centre for Materials Measurement and Technology.

CONTENTS

Page

1 INTRODUCTION 1

2 CURRENT MODELS FOR PREDICTING SPALLATION 1

2.1 MODES OF OXIDE FAILURE 1
2.2 MODELS OF OXIDE BUCKLING 2
2.3 MODELS FOR SPALLATION BY WEDGING 3
2.3.1 Critical Strain Energy 3
2.3.2 Computer Predictions 4
2.3.3 Spallation Maps 6
2.3.4 Prediction of Continued Spallation during Cooling 7

3 STRESS DEVELOPMENT OVER CURVED SUBSTRATES 9

3.1 THERMAL STRESSES 10
3.2 GROWTH STRESSES 11

4 MODELLING SPALLATION FROM CURVED SUBSTRATES 13

5 DIRECTIONS FOR FUTURE WORK 16

6 ACKNOWLEDGEMENTS 17

7 REFERENCES 17

1 INTRODUCTION

In the last decade or so, extensive studies have been undertaken of cracking and the spallation of oxide layers (ref. [1] provides a recent overview). The majority of this work has concentrated on the behaviour of oxide layers on essentially flat surfaces and appreciable progress in understanding behaviour and improving prediction methods has been made for this simple geometry. Whereas such progress is of course welcome and the results can be applied to many industrial applications, it must also be recognised that protective oxide layers are frequently at risk over substrate areas of high curvature. Further work to develop understanding of the mechanical stability of oxides in such situations is necessary in order to develop guidelines for component design and operation.

The purpose of this paper is to highlight concepts important to the consideration of the mechanical stability of oxide layers over curved substrates. By this means, deficiencies in the knowledge base will be identified and directions for future work indicated. In the next section, a review will be given of current understanding of oxide spallation from flat substrates. The influence of surface curvature on thermally-induced stresses will then be considered prior to the more difficult topic of oxide growth stresses over curved surfaces. Possible spallation mechanisms will then be discussed and future research directions indicated.

2 CURRENT MODELS FOR PREDICTING SPALLATION

2.1 MODES OF OXIDE FAILURE

To produce spallation, it is necessary to generate cracks through the oxide layer to the interface at which spallation will occur and also to produce decohesion along that interface. This interface may be one between layers of oxide of different composition, or, indeed, a plane of weakness within a single oxide layer. In the following, it will be assumed that the interface is that between the oxide and metal since this form of failure poses most threat to the endurance of the component. Even though in-plane tensile stresses within the oxide may produce through-thickness cracking, spallation of the oxide layer occurs more readily when the layer is compressively stressed. This reflects common experience that cooling produces most spalled oxide since, for the majority of oxide/metal systems, the oxide then experiences in-plane compressive stresses.

Two distinct processes of spallation of a compressively-stressed oxide have been identified [2]. If the oxide/metal interface has a high *adhesive* strength relative to the *cohesive* strength of the oxide, cracking of the oxide will take place before decohesion whereas poor interfacial adhesion will result in decohesion before oxide cracking. These two distinct routes leading to spallation are shown schematically in Figure 1. When bonding between oxide and metal is strong (Route 1), initial failure of the oxide occurs by compressive shear cracking. Further cooling of the sample results in differential contraction strains which drive wedges of the adjacent oxide layer under the segment bounded by the shear cracks and, thus, produce gradual decohesion at the interface. If interfacial adhesion is poor, eg. due to an aggregation of voids or to the segregation of elements such as sulphur, then compressive straining will initiate buckling of the oxide (Route 2) over these areas of poor adhesion. It may also be possible for individual buckles to spread laterally by propagation of a crack along the interface Figure 1. Spallation results when through-thickness cracks form in regions of high tensile stress within the oxide. These different routes to spallation are termed "wedging" and "buckling", respectively.

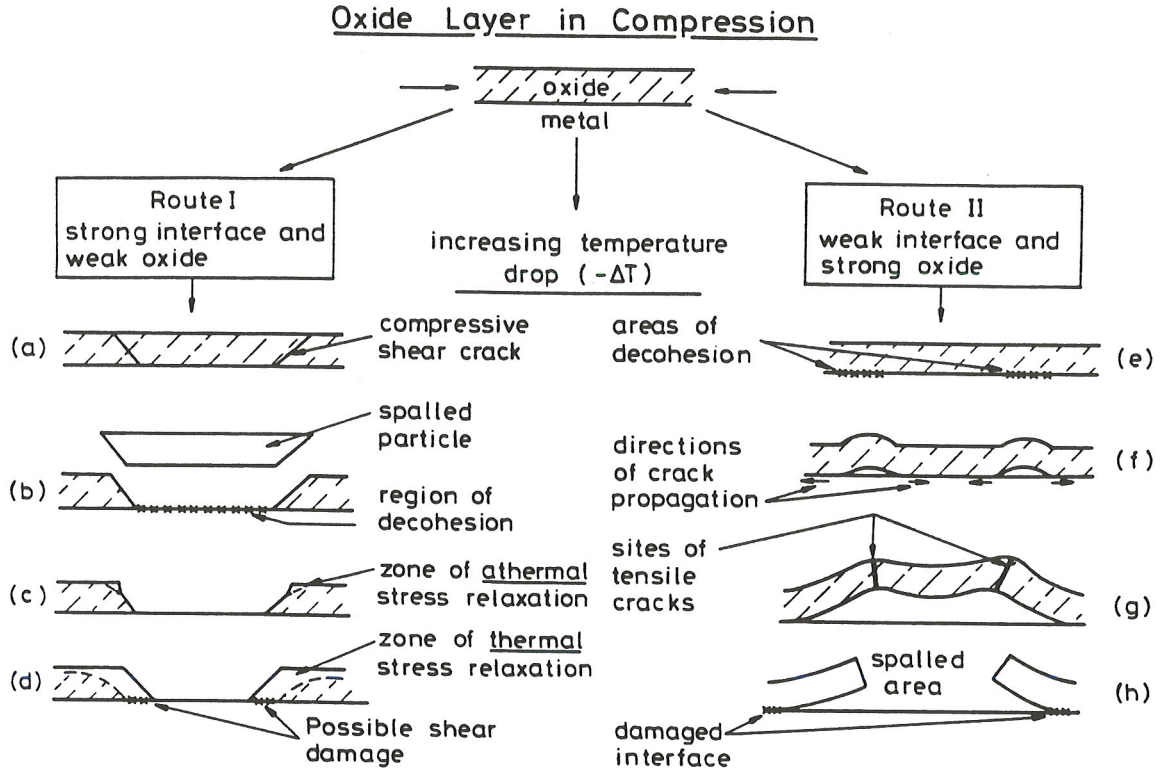


Figure 1: Cracking and spallation caused by compressive oxide stresses.
Route I represents wedge cracking and Route II, buckling failure.

2.2 MODELS OF OXIDE BUCKLING

The critical stress, σ_b, to produce the initial buckle formation, shown schematically on the right-hand side of Figure 1 can be deduced by direct application of elasticity theory [3] as:

$$\sigma_b = \frac{1.22E_{ox}}{(1-\nu_{ox}^2)}\left(\frac{\xi}{R}\right)^2 \qquad (1)$$

which is the solution for a clamped, initially flat oxide layer of thickness ξ overlying a circular area of decohesion of radius, R. If the only source of compressive stress is that deriving from differential thermal contraction, the critical temperature drop, ΔT_b, to initiate buckling is:

$$\Delta T_b = \frac{1.22}{\Delta\alpha(1-\nu_{ox}^2)}\left(\frac{\xi}{R}\right)^2 \qquad (2)$$

where υ_{ox} is the Poisson's ratio of the oxide. On flat specimens the area of decohesion develops during the oxidation process (eg. voidage or contaminant segregation) without the presence of normal stress at the interface. The derivation of these equations also assumes that the oxide deforms only elastically. This is undoubtedly reasonable for refractory oxides such as chromia and alumina which are being cooled from oxidation temperatures of about 0.5 of their melting temperature.

This buckled configuration may produce spallation if the combination of local tensile stress and crack-like defects within the scale can satisfy a critical stress intensity (K_{Ic}) fracture condition. In-plane tensile stresses will occur on the outer surface of the oxide layer at the apex of the buckle and also on the inner surface of the oxide at the periphery of the buckle.

If spallation does not occur immediately as a result of buckle initiation, it may still occur as differential strain accumulates during further cooling either by increasing the deflection of the scale (and hence local tensile stresses) over the same area of decohesion or by propagating the original buckle laterally.

The reason why such propagation should occur can be appreciated from the diagram of Figure 1(f) where the buckle at its periphery acquires the geometry of a conventional tensile crack. Tensile stresses, *normal* to the interface, are thus developed in the residual adherent scale at these positions. The condition for propagation of the buckle is then obtained [4,5] by finding a critical value of R for which further increase will lead to a monotonic reduction in elastic strain energy over and above that energy needed to produce new area of interface. Wells et al. [4] give the critical value of temperature drop, ΔT_{ub}, for such unstable propagation of the buckle as:

$$\Delta T_{ub} = \left[\frac{1.052\xi^4}{R^4} + \frac{1.041\gamma_F}{E_{ox}\xi}\right]^{1/2}\frac{1}{\Delta\alpha} \qquad (3)$$

which can be taken as an upper bound for oxide spallation by buckling. γ_F is here the fracture energy of the interface for the propagation stage. The first term in this expression corresponds to that to initiate the first buckle (equation 2) and the second term, the condition for its propagation.

2.3 MODELS FOR SPALLATION BY WEDGING

2.3.1 Critical Strain Energy

An influential proposal made in 1948 by U. R. Evans [6] was that spallation of part of the oxide layer will occur when the elastic strain energy contained within that volume of oxide equates to the energy required to form new surfaces from the underlying oxide/metal interface. Thus, if W* is the (elastic) strain energy per unit volume of oxide, then the maximum amount available to cause decohesion is:

$$\lambda^2\xi W^*$$

where λ is the spacing between shear cracks (see Route I of Figure 1). Spallation will then occur when

$$\lambda^2 \xi W^* = \lambda^2 \gamma_F \tag{4}$$

where, as before, γ_F is the fracture energy per unit area of interface.

The elastic strain energy term, W*, can be obtained [2] readily for an oxide layer under an equal biaxial compressive stress, σ_{ox}, as:

$$W^* = \frac{\sigma_{ox}^2}{E_{ox}}(1-\nu_{ox}) \tag{5}$$

i.e.

$$W^* = E_{ox}(1-\nu_{ox})(\Delta T)^2(\Delta\alpha)^2 \tag{6}$$

if the only source of stress is differential contraction during cooling from the oxidation temperature. Insertion of equation (6) into (5) gives the critical temperature drop, ΔT_c, to initiate spallation as:

$$\Delta T_c = \left[\frac{\gamma_F}{\xi E_{ox}(\Delta\alpha)^2(1-\nu_{ox})}\right]^{1/2} \tag{7}$$

2.3.2 Computer Predictions

It is important to recognise that the strain-energy condition for failure as initially proposed by U R Evans [6] and extended by Armitt et al. [7] contains no description of how decohesion occurs at the oxide/metal interface, i.e. it contains no cracking *mechanism* and is, thus, a phenomonological approach. The equations derived above cannot be applied to buckling failure since they omit terms accounting for the strain energy involved in the buckle configuration. It is for this reason that Evans and Lobb [2] suggested that they may apply to spallation by wedging. This was recently confirmed [8] by finite element analyses of the wedging mechanism for a chromia layer overlying a thin silica layer on a flat austenitic stainless steel. Figure 2 compares the predicted values of the critical temperature drop, ΔT_c, to initiate spallation as a function of chromia thickness against a spread of experimental measurements of ΔT_c. It can be seen that when the alloy was modelled as creeping, the predictions form a sensible lower bound to the data and show a decrease of ΔT_c inversely with the square root of oxide thickness as required by a critical strain energy criterion (equation 7). However, in the unrealistic case that the alloy deforms only elastically, this criterion does not hold and ΔT_c decreases much more rapidly with increasing oxide thickness.

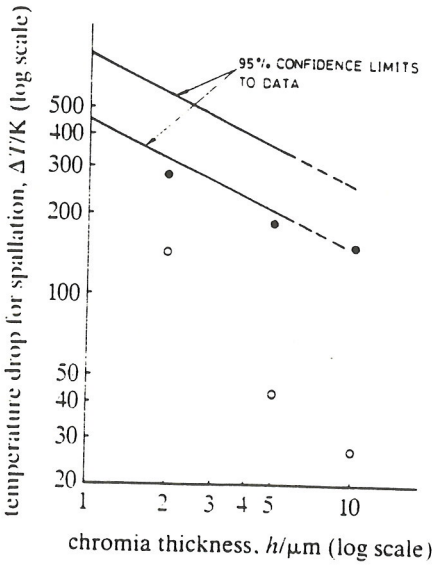


Figure 2: A comparison of computer predictions with the spread of experimental data on the spallation of a chromia layer on an austenitic stainless steel [8].

The validity of the critical strain energy criterion as a tool to predict spallation depends crucially on the kinetics of growth of the interfacial wedge crack. The criterion requires that strain energy accumulates within the oxide layer as temperature drops *but that crack growth does not occur until the spallation temperature is reached.* At this stage in the cooling cycle, it is envisaged that the stored strain energy becomes available to nucleate the shear cracks through the oxide layer and to grow the interfacial wedge crack, essentially instantaneously. Real materials do not usually behave in this way, of course.

Nevertheless, when substrate creep is extensive, i.e. with low cooling rates or a weak alloy substrate, cracking kinetics can approximate to the ideal required of the critical strain energy criterion, as shown in Figure 3. Here, Curve A represents computer predictions [9] for a flat alumina/NiCrAlY coating couple cooled from 1373K at 100K/h. For this example, shear cracking through the oxide (of 5-μm thickness) occurs within a temperature drop of about 150K but crack growth then stops because of creep blunting. Continued cooling during this stage of creep dominance, leads to dissipation of strain energy by substrate creep. At lower temperatures, creep becomes less active and growth of the wedge crack re-commences. This growth phase starts at a temperature drop of about 550K and leads to spallation at about 750K, i.e. wedge-crack growth occupies some 25% of the total temperature drop. Under elastic conditions (Curve C), through-thickness shear cracks again develop at a temperature drop of about 150K but now there is no inhibition of further interfacial cracking and the wedge crack continuously develops with decreasing temperature until spallation occurs at a temperature drop of 260K. In this case, crack growth occupies some 50% of this total temperature drop. Curves B in Figure 3 illustrate the cracking kinetics required by the critical strain energy criterion. Neither is a particularly good fit to the predicted growth curves but, in the creep case, crack blunting and the associated delay in wedge-crack growth after nucleation does mean that the predicted kinetics approximate to the ideal more closely than under elastic conditions. It is not yet known whether this is a general rule but, in applying the strain-energy criterion, it must be borne in mind that it has only been validated (both experimentally and theoretically) for a rather weak, creeping alloy substrate.

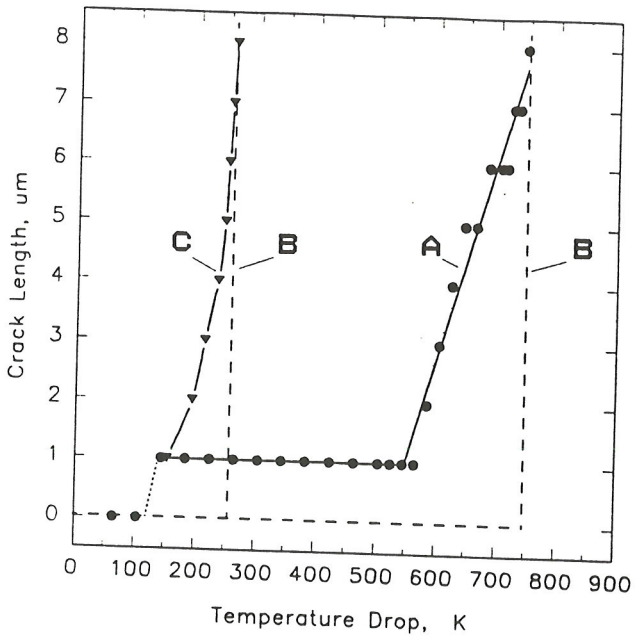


Figure 3: Numerical results of wedge cracking with and without alloy creep for a 5-μm alumina layer on a NiCrAlY substrate [9]. Curves A and C are, respectively, for the alloy deforming by creep or elastically and Curves B represent the ideal cracking implied by the critical strain-energy criterion.

2.3.3 Spallation Maps

The initiation of spallation of oxide from a flat surface during cooling may, in principle, occur by either a buckling or a wedging process (Figure 1). However, the parametric dependence of the temperature drop to effect spallation on oxide thickness varies for each (equations 2, 3 and 7): buckling becomes more diffficult with increasing oxide thickness whereas wedging becomes easier. The relationships between the two mechanisms of failure can readily be appreciated through the use of a spallation map [8]. An example for a chromia layer on an austenitic steel is shown in Figure 4 and clearly illustrates the four regions in which distinctly differing mechanical responses arise to the differential cooling stresses developed within the oxide layer. A detailed discussion of such maps is given elsewhere [1] but an important feature to highlight is the triangular region within which mechanical damage to the oxide is minimal and the oxide layer remains adherent. An additional point to note is that the line representing wedging behaviour is drawn according to equation (7) but with a value of fracture energy, γ_F, of 6 J/m^2. This is higher than would be expected for elastic deformation and indicates a dissipation of cooling strain energy into substrate creep. Indeed, as discussed above, the use of equation (7) cannot readily be supported when deformation is entirely elastic. It should also be noted that this particular value of effective fracture energy is not unique; it will vary with cooling rate, with the temperature range through which cooling occurs and also with the intrinsic creep properties of the substrate. Guidance on the appropriate value to use in any given circumstances should always be obtained from numerical modelling of that particular system or, of course, from experimental results of ΔT_c versus oxide thickness.

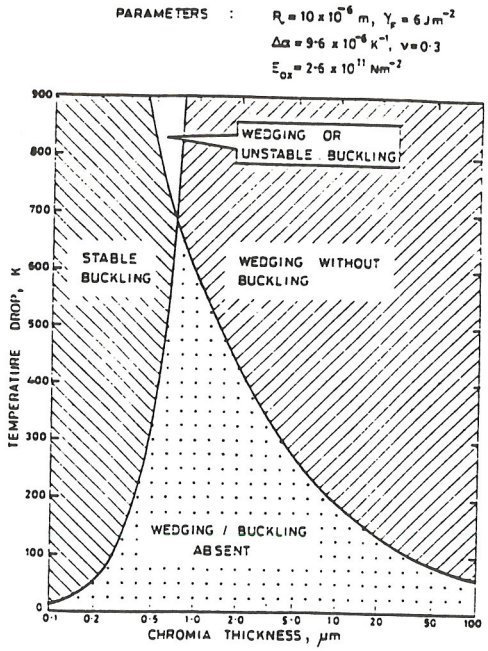


Figure 4: A spallation map for a 20Cr/25Ni steel cooled from 1173K.

2.3.4 Prediction of Continued Spallation during Cooling

It has been known for many years [10] that continued cooling after spallation first occurs results in the release of further spalled oxide. In these early thermobalance tests on a chromia forming austenitic steel, it was found that the quantity of spalled oxide was proportional to the temperature drop over a substantial fraction of the cooling cycle. A further advance in this area was made by Armitt et al. [7] who related the extent of spallation from various Type-316 steel samples to increasing values of the strain energy density. A somewhat different approach was later attempted by Evans and Lobb [11] in which a single specimen was considered to have a distribution of effective fracture energies across its surface. The schematic diagram of Figure 5a shows such a distribution. It is assumed in their treatment that the distribution function is intrinsic to the specimen surface at the start of cooling and is assumed to remain sensibly constant as the temperature drops. The energy requirement for fracture expressed by this distribution is met by the elastic strain energy within the oxide layer produced as a consequence of thermal mismatch strains during cooling. The average value of elastic strain energy increases with temperature drop during cooling and instantaneous values for increasing ΔT are represented by the vertical broken lines shown in Figure 5a. As can be seen, these lines move to the right across the distribution function as cooling proceeds and, so, an increasing fraction of the oxide layer spalls.

Evans and Lobb [11] used a log-normal function to describe their distribution of specific fracture energies and obtained reasonable agreement with the observed increase of spallation with decreasing temperature during the first cooling cycle. A comparison is given in Figure 5(b) and shows satisfactory predictions up to spall fractions of about 40%. At higher fractions, the rate of spallation was found to decrease, an effect which may have been due to stress relaxation within the partially spalled layer (shown schematically for Route I spallation in Figure 1).

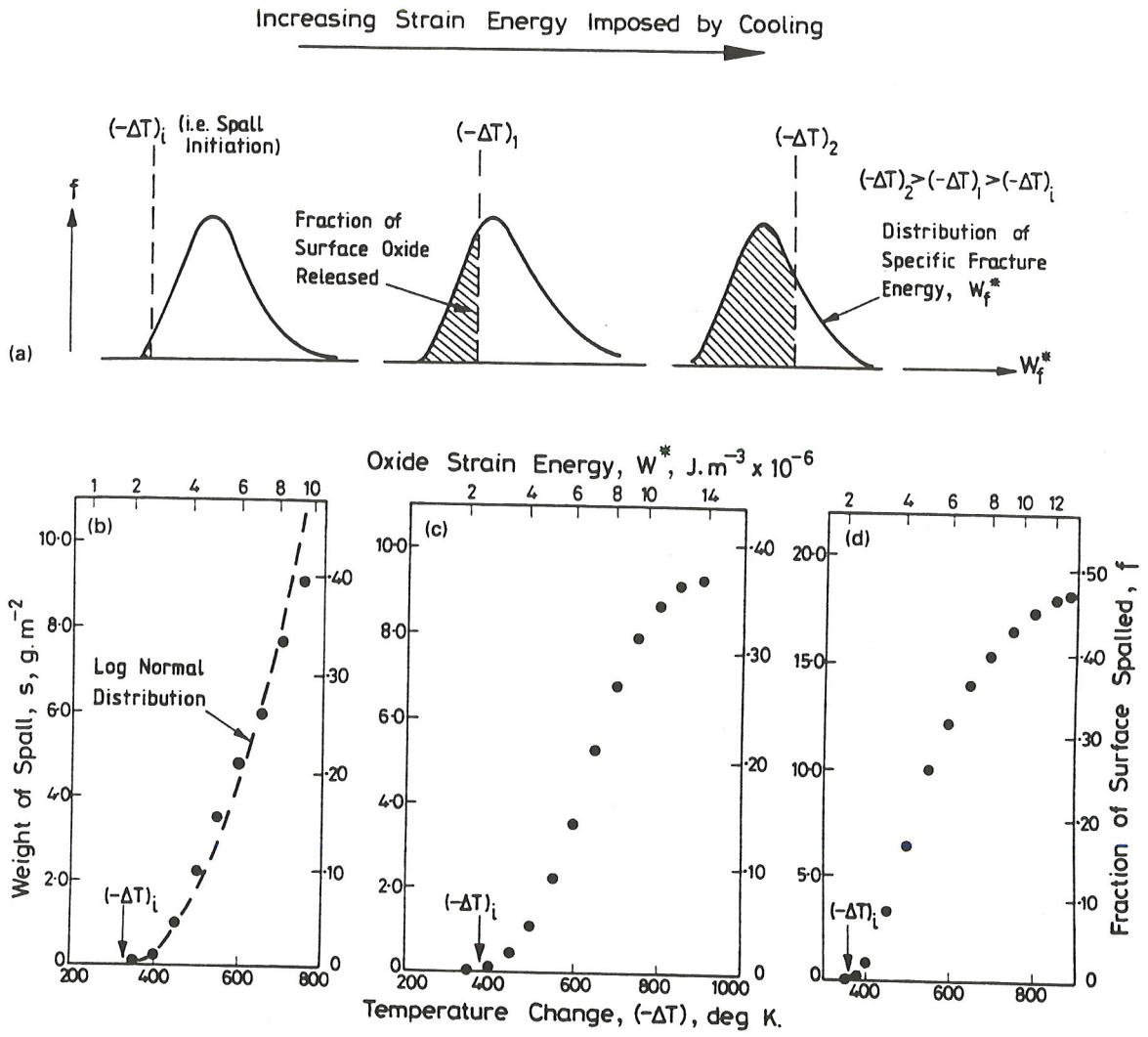


Figure 5: A spatial distribution of the effective fracture energy for spallation leads to continued spallation during cooling: (a) shows the intrinsic distribution; (b)-(d) is the observed fraction of chromia spalled from an austenitic steel during cooling [11].

Moon and Lee [12] have recently adopted this approach but have used simpler mathematics for ease of handling. They also write the spallation condition as:

$$w_g(\Delta T)^2 = \beta\gamma_F \qquad (8)$$

which is equivalent to equation (7) with the constant β containing terms to convert oxide thickness to gross mass gain, w_g. γ_F, the fracture energy, is considered to have a probabilistic distribution as in the Evans-Lobb approach but this is approximated to give the fraction, F, of oxide spalled as:

$$F = \left[\frac{w_g(\Delta T)^2}{\beta} \right]^m \qquad (9)$$

where m is a constant of order unity. Moon and Lee find good agreement with experimental data for chromia on IN825 and IN601 and for alumina on TD601; the results for the chromia-forming IN601 alloy are shown in Figure 6.

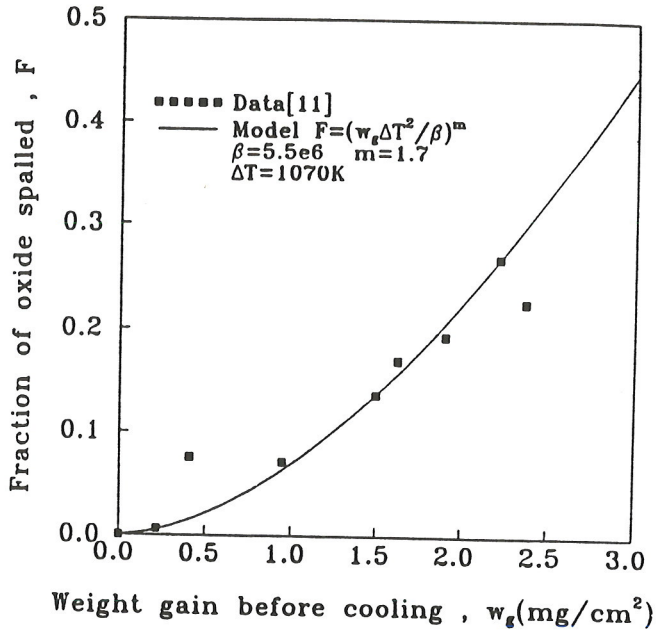


Figure 6: Observed fraction of the chromia layer spalled from IN601 and comparison with equation 9 [12].

Another recent approach to this problem of continued spallation is that of Zhang and Shores [13] who again make use of the concept of a distribution of fracture strengths across the specimen surface. In their tests, samples of Type-304 steel were oxidised for short periods (20 h) at 1073K to give scale thicknesses of about 3 μm and spallation occurred by a buckling route (Figure 1). The failure process was envisaged to be the propagation of a buckle across the sample surface , i.e. unstable buckling, with a distribution of properties reflecting a distribution in radius of interfacial zones of initial decohesion. This is an interesting approach to explain continued spallation by buckling but the treatment given by Zhang and Shores is valid only for elastic deformation and sharp cracks. It would require further development before being applied to a creeping substrate.

3 STRESS DEVELOPMENT OVER CURVED SUBSTRATES

The above discussion on oxide spallation from flat surfaces has concentrated on compressively stressed oxide layers within which oxidation growth stresses are negligible. This is a simplifying assumption but one that accords with reality in many cases [1]. The situation may differ with curved substrates, however, since there is greater opportunity for fresh oxide to form under geometrically constrained conditions. In this section, therefore, both thermal and growth stresses will be considered separately.

3.1 THERMAL STRESSES

The differential cooling strains that are produced during temperature changes result in a planar biaxial stress distribution within the oxide layer formed on an ideally flat surface. In the absence of oxide cracks or edge effects, there are no normal stresses across the oxide/metal interface. The situation is fundamentally different for a curved substrate. An important example is the cooling of a circular cylinder, the outer surface of which has an oxide layer of lower thermal expansion coefficient than that of the substrate. During cooling, the substrate contracts more than the oxide so that radial tensile stresses are generated across the interface in addition to in-plane compressive stresses within the oxide layer. Provided the oxide layer is thin, the tensile stress across the interface is approximated by:

$$\sigma_r = \frac{\Delta\alpha\Delta T E_{ox}\xi}{(1-\nu_{ox})a} \qquad (10)$$

where a is the radius of the cylinder, ξ is the oxide thickness, $\Delta\alpha$ is the difference between metal and oxide expansion coefficients and $\Delta T=T_{ox}-T$ where T_{ox} is the oxidation temperature and T is the temperature at which σ_r is evaluated. ΔT is positive for cooling conditions and so the stress normal to the interface is tensile, as anticipated. Representative values of the parameters for a chromia/austenitic steel system are: $\Delta\alpha=9.3\times10^{-6}$ K^{-1}; $E_{ox}=260$ GPa; $\nu_{ox}=0.3$; $\xi=5\times10^{-6}$ m; $a=0.0075$ m which, from equation (10) predicts a tensile stress of about 0.9 MPa for a temperature drop of 400 K. For the same example, the in-plane (tangential) oxide stresses are given approximately as:

$$\sigma_\theta = -\frac{\Delta\alpha\Delta T E_{ox}}{(1-\nu_{ox})} \qquad (11)$$

which, to first order, is independent of oxide thickness and the radius of curvature of the substrate. With the same parameters as above, it can be seen that in-plane compressive stresses of some 1380 MPa are developed for the temperature drop of 400 K.

Equation (11) is identical to the equivalent for a flat specimen [14] and serves to show that the same in-plane stresses would be developed in each case. The difference with the curved geometry is the presence of a small normal stress across the oxide/metal interface. It will be shown later that this has negligible influence on the spallation behaviour for this particular example. On the other hand, for notionally flat specimens, it is the *local* curvature which is important so that regions such as corners or surface irregularities such as machining marks or undulations on sprayed coatings can experience large stresses. As a first approach to evaluating these it is reasonable to use equations (10) and (11) since the thermal contraction of the substrate regions of local curvature tend to be determined by the large bulk of the underlying substrate and will not be much influenced by the oxide layer. This is the key requirement for the valid use of the "thin-oxide" equations given above.

The signs of these stresses change with the sign of the product $\Delta\alpha\Delta T$. Thus, cooling of a 2¼Cr/Mo steel cylinder with a layer of magnetite on the outer surface, will result in a compressive radial stress across the interface and tensile in-plane stresses within the oxide layer [15] simply because magnetite has a larger expansion coefficient than the steel. In more complex systems where multilayer scales develop, similar equations to the above can be used for each oxide layer [16].

For concave substrates, equations (10) and (11) still apply but the signs of the stresses may differ from the case of convex curvature. A simple, if not entirely rigorous approach, is to treat the concave cylindrical radius, a, as negative. Thus, equation (10) would predict a compressive stress across the oxide/metal interface on the concave surface of the cylinder

during cooling (for $\alpha_{metal}>\alpha_{oxide}$) and that equation (11) (which does not contain the parameter *a*) shows, just as in the case of convex curvature, that the in-plane tangential stress is compressive.

For spherical, rather than cylindrical substrates, the same sense of stress exists as described above but, for a given radial stress σ_i, the in-plane tangential stress is:

$$\sigma_\theta = \frac{\sigma_r a}{2\xi} \qquad (12)$$

This is half the value obtained from equations (11) and (12) for a cylindrical substrate. In each case, though, an adequate guideline is that significant differences from the spallation behaviour of flat surfaces will arise when the oxide thickness is of the same order as the underlying radius of curvature. In this situation, the radial stress across the oxide/metal interface is of similar magnitude as the tangential, in-plane stress within the oxide layer and would be expected to produce significant perturbation of the growth kinetics of the interfacial crack.

3.2 GROWTH STRESSES

The above discussion on thermal stresses has implied that the growth stresses at the oxidation temperature are negligible. As pointed out earlier in the discussion of spallation from flat surfaces, this often seems to be an adequate simplification, particularly in systems in which oxide growth occurs by cation diffusion and also for thin-sectioned samples in which relaxation of growth stresses can occur by metal creep. Indeed, even when oxide growth occurs by anion diffusion, it is feasible for cooperative diffusion in the substrate to create space for the formation of new oxide [17-19]. It is clear that models of stress development which assume creep or diffusional rigidity [20] are inadequate and unlikely to predict reliable levels of growth stresses.

The situation may be fundamentally different during the oxidation of curved substrates since fresh oxide, even that growing by cation diffusion, may have to be produced under constrained conditions leading to substantial levels of growth stress. This is an area of the subject which is poorly understood mechanistically although qualitative understanding is well developed [21,22]. The various combinations of oxide growth mechanisms and sense of surface curvature will lead to differing oxide stress states, as summarised by Hancock [21] in Figure 7.

For oxides growing by cation diffusion, new oxide is formed at the outer surface of the oxide layer and the underlying metal will retreat if the cation vacancy flux (if appropriate) is annihilated at the oxide/metal interface. In order to maintain continuity at this interface, the oxide scale needs to be "glued" onto the alloy substrate. This process causes a tensile resultant force normal to this interface for both convex and concave surfaces. In addition, for the former geometry, compressive in-plane normal stresses are produced throughout the oxide layer (Figure 7(i)). These stresses can result in compressive shear failure, if oxide/metal adhesion is strong so that it is conceivable for wedge-crack growth to occur at the oxidation temperature as a result of the growth stresses. For concave surfaces, the same oxidation mechanism will tend to form tensile in-plane stresses which will be greatest at the inner oxide surface and may result in tensile cracking (Figure 7(ii)).

When oxides grow predominantly by anion diffusion, fresh oxide forms at the base of the oxide at the oxide/metal interface and this changes the stress systems developed on the two substrate geometries. Thus, on a convex substrate, the outer (older) regions of the oxide layer need to be increased in length as fresh oxide is formed at the interface. The tangential (i.e. in-plane) stresses will accordingly vary from compression near the oxide/metal interface to tension near the outer surface. Tensile cracks may be produced in these outer regions

(Figure 7(iii)). On a concave substrate, the tangential stresses are compressive throughout the oxide (Figure 7 (iv)) and the normal stress across the interface is also compressive.

The distribution and sign of the oxide growth stresses described by Hancock [21] and shown in Figure 7 are qualitatively plausible but do not provide a route for the calculation of the *magnitude* of these stresses. The simplest approach, of course, is to treat the oxide and metal as elastic [23] and ignore stress relaxation from creep or from the diffusional provision of space at the oxide/metal interface. Such an analysis will inevitably provide overestimates of oxide growth stresses. A more satisfying initial approach is that of Manning [22] who calculates the scale displacement rate required to maintain contact with the substrate for conditions in which the oxide grows by a combination of anion and cation diffusion and for which the metal consumed in the oxidation process may arise from both the oxide/metal interface and from locations within the substrate. Manning's approach recognises many of the subtleties of the problem but, again, cannot readily be used to predict the magnitude of growth stresses simply because stress relaxation processes are difficult to quantify.

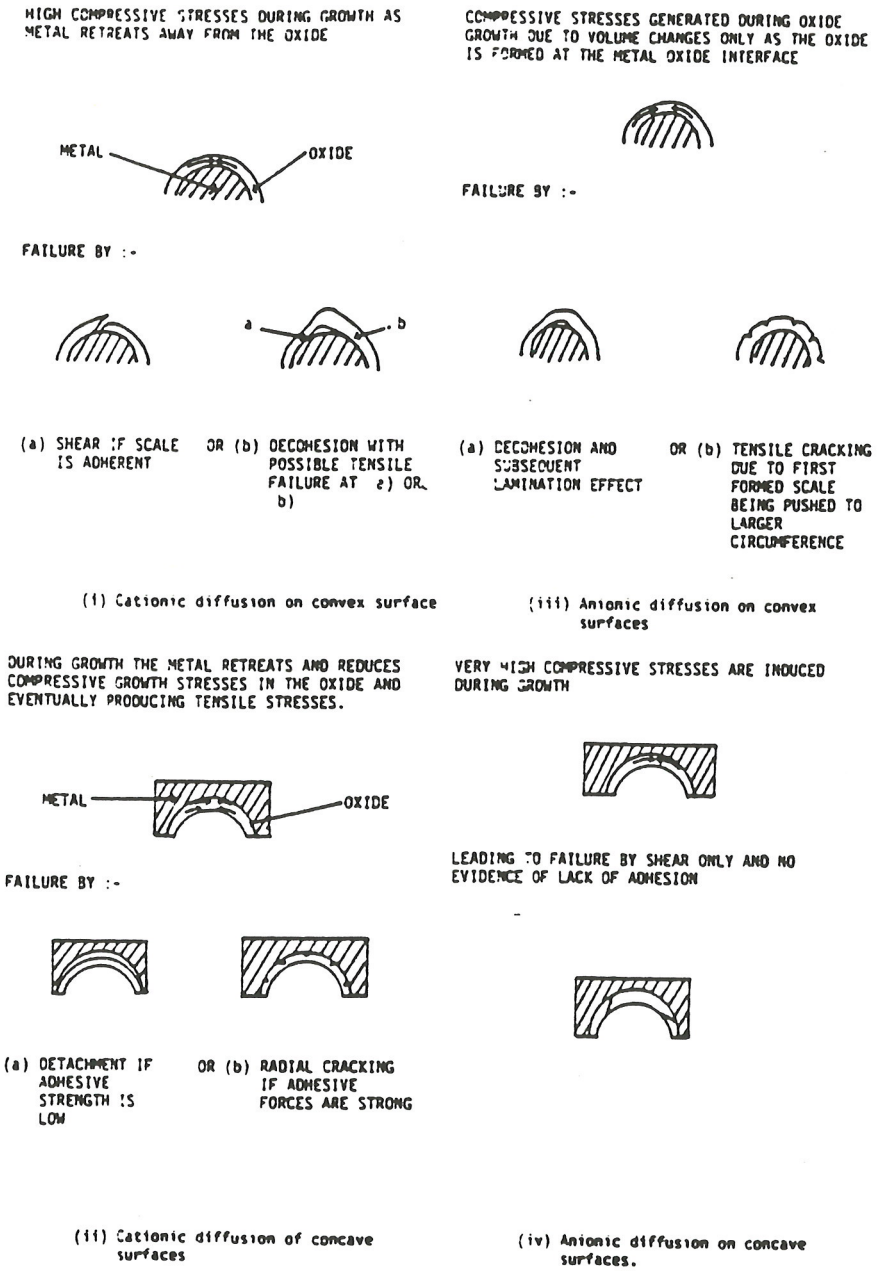


Figure 7: Growth Stresses and Possible Failure Modes on Curved Substrates [21]

4 MODELLING SPALLATION FROM CURVED SUBSTRATES

For thin oxides, the important difference in the stress systems between flat and curved substrates is the presence, in the latter case, of a radial normal stress across the oxide/metal interface. This stress may be tensile or compressive and can orignate from both the oxidation process and during temperature changes. Under circumstances where the in-plane oxide stress is compressive, e.g. during cooling of convex geometry with $\alpha_{metal} > \alpha_{oxide}$, the oxide spallation mode may well be by wedging as shown schematically in Figure 8.

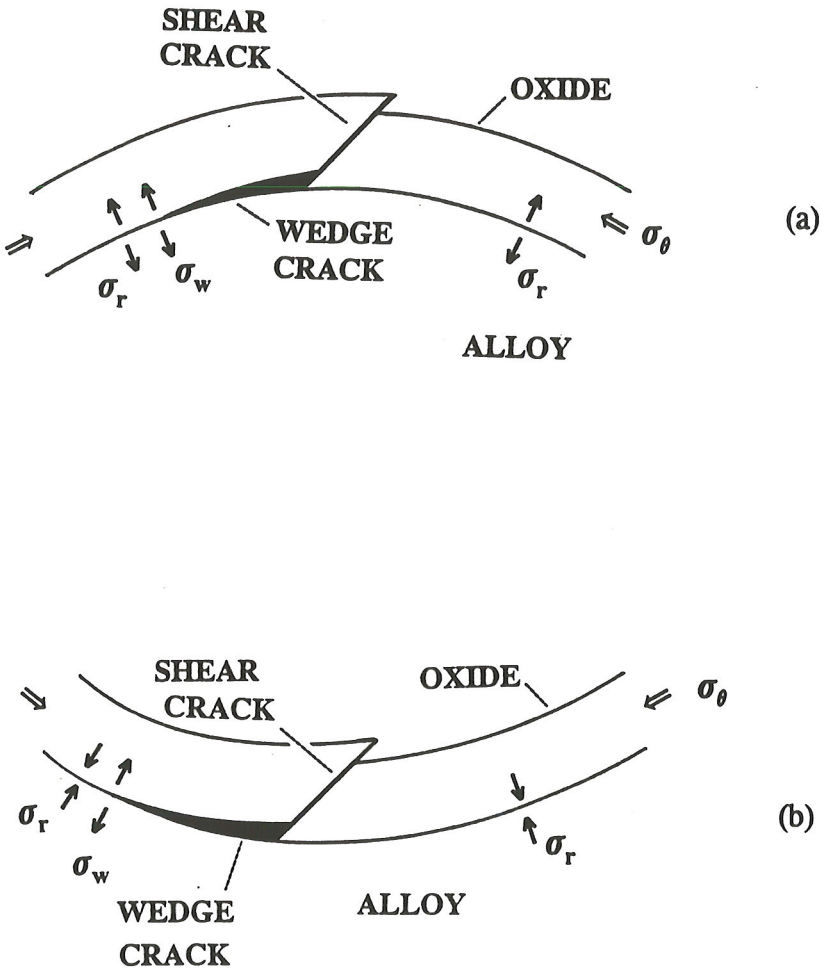


Figure 8: Normal Stresses across the Oxide/Metal Interface ahead of a Wedge Crack on (a) Convex and (b) Concave Substrates.

It can be appreciated that a tensile stress across the interface in addition to that developed at the tip of the wedge crack due to the wedging action will increase the crack's growth rate and, thus, produce a lower ΔT_c than that for a flat substrate. For thin oxides on concave substrates, the greater contraction of the substrate during cooling will produce compressive normal stresses across the oxide/metal interface and these will tend to retard the cracking process. The nett effect will be an improvement in spallation resistance.

At this stage of understanding, however, no quantitative (numerical) modelling, that allows for creep relaxation, has been undertaken for curved substrates and no estimate can be made of the magnitude of these changes in ΔT_c. It is anticipated that, as in the case for flat

specimens, the influence of substrate creep will dominate the crack-growth kinetics and will determine whether the critical strain-energy criterion is an acceptable description of the spallation process.

There is a similar shortfall in experimental measurements of ΔT_c on curved substrates. The most extensive study has been conducted [11] on a chromia-forming 20Cr/25Ni steel and produced the results given in Figure 9. This provides a comparison between observed values of ΔT_c, found on cooling from 1123K, for flat specimens and tubes of approximately 15 mm diameter. The data are well described by the critical strain-energy criterion (equation 7) as shown by the solid line but there is no significant difference between the specimen geometries. This should not be too surprising, however, since the calculated tensile normal to the oxide/normal interface is, as was shown in Section 3.1, <1 MPa and some 10^{-3} of the in-plane compressive stresses developed during cooling.

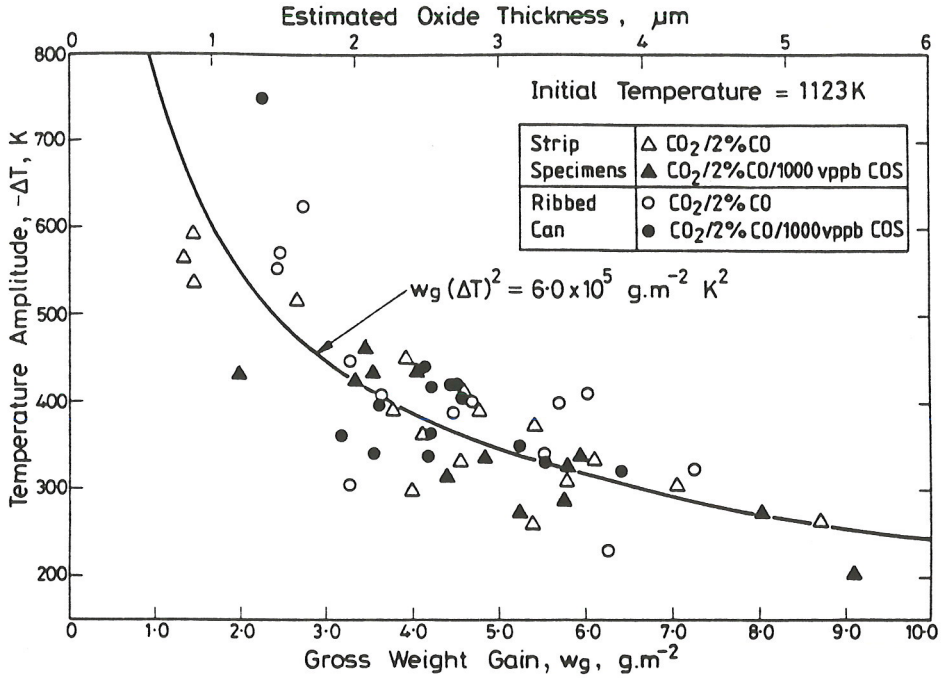


Figure 9: Variation of ΔT_c with Gross Weight Gain or Oxide Thickness for Chromia Spallation from 20Cr/25Ni Steel Specimens of differing Geometries [11].

Much higher levels of curvature can be present above *local* surface irregularities. Thus, in a recent study, Strawbridge et al. [24] have studied the spallation during cooling of a porous, post-breakaway Ni-rich oxide for which delamination failures were found to occur above nodules on a plasma-sprayed NiCrAlY coating. Since failure occurred within the oxide it was reasonably assumed that elastic conditions obtained and that scale fracture could be described by linear elastic fracture mechanics. The basis of the Strawbridge model is shown in Figure 10 in which the tensile stress across the oxide/metal interface is envisaged to produce propagation of a pre-existing void near the interface but within the oxide layer.

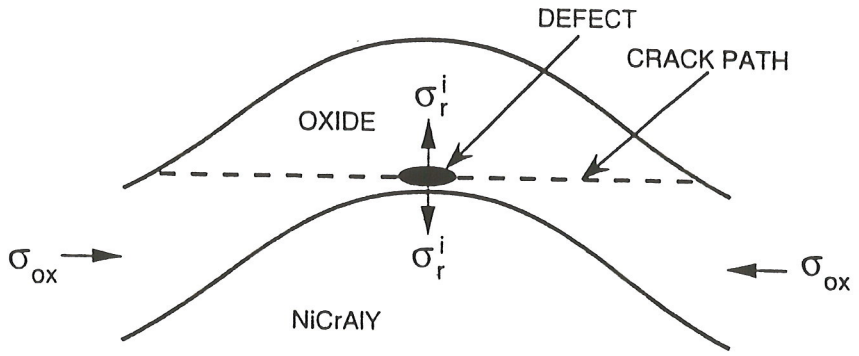


Figure 10: Propagation of an Oxide Defect near a Convex Oxide/Metal Interface [24].

The critical temperature drop, ΔT_c, to produce spallation is given in their model as:

$$\Delta T_c = \frac{K_{1c} R (1-\nu_{ox})}{2E_{ox}(\pi a)^{1/2}(\alpha_{metal}-\alpha_{oxide})\xi} \qquad (14)$$

if growth stresses can be neglected. Here, K_{1c} is the critical stress intensity factor = 1.6 $MNm^{-3/2}$ for NiO [25], α_{metal}-α_{oxide}=2.5x10^{-6} K^{-1}, E_{ox} is the Young's modulus of the oxide (NiO) and taken as 190 GPa, ν_{ox}=0.3 is the Poisson's ratio for the oxide, R=50 μm is the measured radius of curvature, (2*a*)=10μm is the largest measured void on the fracture plane and ξ is the local oxide thickness. It should be noted that the model predicts a dependence of ΔT_c on ξ^{-1} rather than on $\xi^{-½}$ expected from a wedging process (equation 7) on a creeping substrate. This prediction, using the above values for the various parameters, is shown as the solid line in Figure 10. The experimental results shown on this figure are thermobalance measurements and, although these are characteristically scattered, the theoretical line obviously provides a reasonable description to the data, as evidenced by its proximity to the dotted line which represents a statistical best fit.

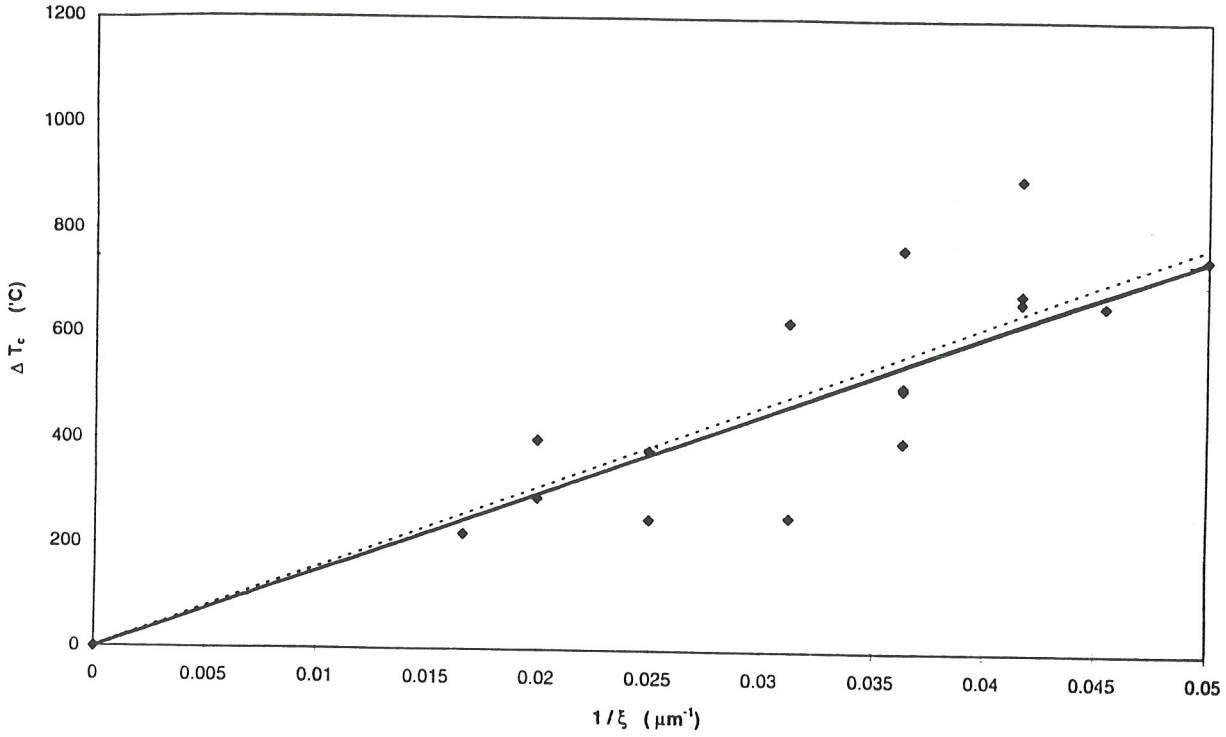


Figure 11: Comparison of Model Predictions (solid line) with Best Fit (broken line) and Thermobalance Results of Spallation of a Porous Ni-rich Oxide from a NiCrAlY Coating [24].

5 DIRECTIONS FOR FUTURE WORK

It has become clear during this review that the ability to model and, hence, predict oxide spallation from curved substrates lags considerably behind that for flat substrates. The situation is aggravated by the paucity of experimental data, not only on spallation kinetics during cooling but also on the development of growth stresses on curved specimens. The directions of future work need to address these fundamental issues as indicated below:

- measure growth stresses on curved substrates and relate to the direction of oxide growth and the sense and radius of surface curvature;
- determine the critical temperature drop to initiate spallation for various curvature parameters;
- measure the kinetics of continued spallation after initiation for both senses of curvature and various radii;
- incorporate new experimental data into modelling algorithms (e.g. a critical strain-energy criterion) and attempt numerical modelling of the spallation process.

6 ACKNOWLEDGEMENTS

This work was carried out as part of the 'Environmental Degradation Programme': a programme of underpinning research funded by the UK Department of Trade and Industry.

7 REFERENCES

1. H E Evans; Intnl. Mater. Rev., 1995, **40**, 1.
2. H E Evans and R C Lobb; Corros. Sci., 1994, **24**, 209.
3. S Timoshenko; "Theory of Elastic Stability", McGraw-Hill, New York, 1936, p367.
4. C H Wells, P S Follansbee and R R Dils; in "Stress Effects and the Oxidation of Metals", ed J V Cathcart, AIME, New York, 1975, p220.
5. A G Evans and J W Hutchinson; Intnl. J. Solids Struct., 1984, **20**, 455.
6. U R Evans; "An Introduction to Metallic Corrosion", Edward Arnold, London, 1948, p195.
7. J Armitt, D R Holmes, M I Manning, D B Meadowcroft and E Metcalfe; "The Spallation of Steam Grown Oxide from Superheater and Reheater Tube Steels", Report FP-686, Electric Power Research Institute, Palo Alto, California, USA, 1978.
8. H E Evans, G P Mitchell, R C Lobb and D R J Owen; Proc. Roy. Soc., 1993, **A440**, 1.
9. H E Evans, A Strawbridge, R A Carolan and C B Ponton; unpublished work.
10. J M Francis, M T Curtis and D A Hilton; J. Nucl. Mater., 1971, **41**, 203.
11. H E Evans and R C Lobb; Proc. "EUROCORR 87", Dechema, Frankfurt, 1987, p135.
12. Chang-Oh Moon and Soon-Bok Lee; Oxid. Met., 1993, **39**, 1.
13. Yifan Zhang and D A Shores; J. Electrochem. Soc., 1994, **141**, 1255.
14. J K Tien and J M Davidson; in "Stress Effects and the Oxidation of Metals", ed J V Cathcart, AIME, New York, 1975, p200.
15. W Christl, A Rahmel and M Schütze; Oxid. Met., 1989, **31**, 1 & 35.
16. E Metcalfe and M I Manning; "The Spalling of Steam Grown Oxide from Austenitic and Ferritic Steels", Report RD/L/R1966, CEGB, 1977.
17. H E Evans, D J Norfolk and T Swan; J. Electochem. Soc., 1978, **125**, 1180.
18. A Atkinson and D W Smart; J. Electrochem. Soc., 1988, **135**, 2886.
19. J Robertson and M I Manning; Mater. Sci. Technol., 1988, **4**, 1064.
20. A G Evans, G B Crumley and R E Demaray; Oxid. Met., 1983, **20**, 193.
21. P Hancock; in "Environmental Degradation of High-Temperature Materials", The Institution of Metallurgists, London, 1980, p2/1.
22. M I Manning; in "Corrosion and Mechanical Stress at High Temperatures", eds V Guttmann and M Mertz, Applied Science Publishers, London, 1981, p323.
23. V Rosenband and A Gany; Corros. Sci., 1995, **37**, 1991.
24. A Strawbridge, H E Evans and C B Ponton; paper to be presented at the "Fourth International Synposium on High Temperature Corrosion", Les Embiez, 1996.
25. S R J Saunders, W T Evans and D J Hall; Corros. Sci., 1993, **35**, 965.